3D printed denture bases resins: Glazing as an alternative to improve surface, mechanical and microbiological properties

Ana Larisse Carneiro Pereira,[a] João Pedro dos Santos Silva,[b] Manassés Tercio Vieira Grangeiro,[c] Annie Karoline Bezerra de Medeiros,[d] Marcos Antonio Bottino,[e] Valentim A. R. Barão,[f] Adriana da Fonte Porto Carreiro[g]

[a]DDS, MSc, PhD Candidate, Department of Dentistry, Federal University of Rio Grande do Norte (UFRN), Natal, Rio Grande do Norte, Brazil. E-mail: larisse.c89@gmail.com

[b]DDS, MSc, PhD Candidate, Department of Prosthodontics and Periodontology, Piracicaba Dental School, Universidade Estadual de Campinas (UNICAMP), Piracicaba, São Paulo, Brazil. E-mail: jpedrooss85@gmail.com

[c]DDS, MSc, PhD, Department of Dental Materials and Prosthodontics, São Paulo State University (UNESP), São Paulo, Brazil. E-mail: terciomanasses@gmail.com

[d]DDS, MSc, PhD, Department of Dentistry, Federal University of Rio Grande do Norte (UFRN), Natal, Rio Grande do Norte, Brazil. E-mail: annie_medeiros@hotmail.com

[e]Professor, Department of Biomaterials, Dental Materials, and Prosthodontics, Institute of Science and Technology, São Paulo State University (UNESP), São José dos Campos, Brazil. E-mail: mmbottino@uol.com.br

[f]Associate Professor, Department of Prosthodontics and Periodontology, Piracicaba Dental School, Universidade Estadual de Campinas (UNICAMP), Piracicaba, São Paulo, Brazil.

[g]Full Professor, Department of Dentistry, Federal University of Rio Grande do Norte (UFRN), Natal, Rio Grande do Norte, Brazil. E-mail: adriana.carreiro@ufrn.br

Corresponding author:

Dr Adriana da Fonte Porto Carreiro

Department of Dentistry, Federal University of Rio Grande Do Norte (UFRN), Avenida Senador Salgado Filho, nº 1787, Zip Code: 59056000, Natal, Rio Grande do Norte, Brazil. Electronic address: adriana.carreiro@ufrn.br

ABSTRACT

Objective: Evaluate the impact of glazing denture base resins (heat-polymerized and 3D printed) on surface, mechanical and microbiological properties.

Methods: Discs (10×3 mm) and bars (64×10×3.3±0.2 mm) were manufactured using heat-polymerized denture base resin (CT) and 3D printed denture base resin (Yller [YL], Prizma [PZ] and PrintaX [PX]). All resin types underwent surface polishing and were divided into two groups: unglazed and glazed. The following were evaluated: roughness (Ra), wettability (º), brightness (GU) and electron scanning microscopy, as well as microbiological analysis (Streptococcus mitis and Candida albicans dual-species biofilms) and Knoop microhardness was conducted on discs (n=10). Meanwhile, flexural strength testing (n=20) was performed on the bars. Half of the specimens subjected to surface and mechanical characterizations were thermocycled (10,000 cycles). Mann-Whitney test ($p<0.05$) and simple and multiple linear regression analysis ($p<0.20$) were employed to evaluate the impact of glazing on denture base resins.

Results: The application of glaze led to a reduction in roughness by -0.33 µm and wettability by -8.47º, while increasing brightness by 21.30 (GU) ($p<0.001$) for 3D printed resins compared to CT. After thermocycling, there was an increase in Ra and a decrease in wettability and brightness ($p<0.05$). Glaze increased hardness without a negative impact from thermocycling ($p<0.001$) and increased flexural strength for PZ compared to CT ($p<0.001$). C. albicans colonization decreased by -7.79 log CFU/mL for 3D printed resins in mixed biofilm compared to CT ($p<0.05$).

Significance: The application of glaze resulted in smoother, brighter, and harder surfaces for the 3D printed resins, while also reducing biofilm colonization.

Keywords: complete denture, coatings, 3D printing, polymers, additive manufacturing, digital denture.

1. Introduction

One of the significant challenges affecting dental prostheses is the abrasive wear incurred during both function and cleaning processes. As a result, surface hardness is compromised, thereby exacerbating mechanical and chemical wear of the denture base resin [1-3]. This deterioration provides a favourable environment for fungal and bacterial colonization, which are implicated in various oral diseases, including denture stomatitis and oral candidiasis [4]. Moreover, elderly individuals, who often exhibit diminished manual dexterity, struggle with effectively removing plaque build-up on dental prostheses, rendering them even more vulnerable to oral infections [4].

The polishing of the denture base resin reduces the presence of defects such as scratches and consequently, the surface roughness. Various techniques have been used to polish the materials used to make prosthesis. Conventionally, after finishing with drills and abrasive stones, a polish is obtained with water and fine pumice stone, polishing paste or liquid polish containing aluminum oxide particles. Recently, surface sealing agents have been introduced to minimize porosity surface and obtain smooth surfaces, as well as fill surface defects, increase wear resistance and provide better resistance to stains [5-7].

In terms of composition, the glazes contain nanoparticles (Nanoverniz; anax USA, Ardmore, OK and Optiglaze; GC America Inc, Alsip, IL), primarily composed of silica (SiO_2) or titanium dioxide (TiO_2) [8]. The incorporation of silica nanoparticles (SiO_2) not only increases the surface resistance of the resin but also imparts a low surface energy characteristic, making it challenging for biofilms to adhere [9]. On the other hand, titanium dioxide (TiO_2) contributes to improvements in the elastic modulus and hardness of the denture base resin. The unique photoactive properties of TiO_2 nanoparticles, combined with their superior mechanical characteristics, establish them as pivotal additives for enhancing the performance of polymeric materials [9,10].

Based on this information, light-curing glazes have been developed and applied to the surface of 3D printed denture base resin to effectively seal pores and diminish surface roughness [1,2]. To compare heat-polymerized and 3D printed denture base resins, analysis of biofilm, flexural strength, surface hardness, wettability and surface roughness were performed [11-13]. The studies revealed that 3D printed denture base resin exhibited lower flexural strength and surface hardness compared to heat-polymerized denture base resin and CAD-CAM (milled) specimens [11,12]. Additionally, increased adhesion of *Candida albicans* was observed on 3D printed denture base resin discs versus heat-polymerized denture base resin and CAD-CAM (milled) specimens [12,13]. However, no study to date has investigated the surface, mechanical, and microbiological properties of 3D printed denture base resin after undergoing glazing.

Given the above information, the introduction and widespread adoption of additive manufacturing over the past three decades have revolutionized the production of prostheses, enabling faster fabrication compared to traditional methods. This advancement has not only facilitated a more rapid manufacturing process but has also promoted cost-effectiveness and reduced waste, particularly in comparison to prostheses manufactured using CAD-CAM resins (milled). However, despite the benefits of additive manufacturing, there remains a need to enhance the properties of 3D printed denture base resins to improve their clinical longevity and enhance patient aesthetic satisfaction. Hence, this study aims to assess the impact of glazing on denture base resins (heat-polymerizable and 3D printed), focusing on surface, mechanical, and microbiological properties.

2. Materials and methods

The experimental design (Figure 1) and the materials used (Table 1) in the present study are detailed. Disc-shaped (10×3 mm) [12] and bar-shaped (64×10×3.3±0.2 mm) specimens were manufactured according to ISO 20795-1:2013 [14], in heat-polymerized (CT Group) and 3D printed (Yller [YL], Prizma [PZ] and PrintaX [PX]) denture base resins.

2.1 Specimen preparation

Metallic matrices were manufactured in both disc and bar shapes, in the previously specified configurations. To create casts, two-thirds (2/3) of the muffle was filled with type III plaster, while the remaining space was filled with condensation silicone. Subsequently, the metallic matrices were inserted into the condensation silicone, effectively forming casts. These casts were filled with a heat-polymerized denture base resin using a ratio of 14 g of powder for 6.5 mL of liquid. The acrylic resin was poured into the plaster cast, which was isolated with a water-soluble alginate solution (Cel Lac; S.S. White). A polyethylene sheet was positioned over the resin, and an initial pressure of 850 kgf was applied for 5 min, followed by a final pressure of 1,250 kgf for 20 min. The classic acrylic resin polymerization procedure was carried out in an automatic device

(Thermotron; Thermotron Dental Products), set to a water cycle heated to 74°C for 9 h [15].

The printed denture base resin specimens were designed using CAD software (Autodesk; Meshmixer) and saved as STL (Standard Tessellation Language) files. These files were then printed (Anycubic Photon Mono SE), with the following settings: YL (layer thickness: 0.05; exposure time [s]: 3.50; off time [s]: 1.00; bottom exposure time: 40; layers: 4), PZ (layer thickness: 0.05; exposure time [s]: 6.5; off time [s]: 1.00; bottom exposure time: 80.00; layers: 8), PX (layer height: 0.05; quantity of fixing layer: 6; base exposure time: 30 seconds; normal exposure time: 4 seconds). Following printing, the denture base underwent post-processing, which involves washing in isopropyl alcohol [YL: 10 minutes, PZ: 5 minutes; PX: 10 minutes] and post-curing [YL: 10 minutes, PZ: 20 minutes; PX: 10 minutes]).

2.2 Surface glazing

Initially, the surface of the resin specimens underwent a polishing procedure, following a previous protocol [16]. In summary, 0.2 g of aluminum oxide paste (Universal Polishing; Ivoclar Vivadent AG) was applied to one side of the specimens with a felt wheel (MSH78M; American Burrs) coupled to a polishing motor (3000 rpm) (300B; MicroNX). Polishing was precisely timed with a digital stopwatch, starting when the felt wheel touched the specimen and lasting for 30 seconds. After polishing, the specimens were ultrasonically washed in 2 cycles of 10 minutes each in distilled water to remove the polishing paste, and then allowed to dry at room temperature [16]. A thin layer of glaze (Megaseal; OdontoMega) was applied to the surface of the specimens using a soft brush, applying gentle strokes in one direction to prevent the formation of bubbles. The glaze was left on the surface for 20 seconds before polymerization, after which the specimens were placed in a post-curing machine for 5 minutes. Subsequently, all specimens were stored at 37ºC immersed in distilled water until tests were carried out.

2.3 Thermocycling

Half of the specimens (n=10) subjected to surface and mechanical characterizations underwent thermocycling (OMC 300 TSX; Odeme Dental Research) which consisted of water baths at temperatures of 5 ±1ºC and 55 ±1°C, with a dwell time of 30 seconds in each bath and 2 seconds out of the water between baths, for a total of 10,000 cycles [17].

2.4 Surface characterization

2.4.1 Surface roughness

Surface roughness measurements (n=10) were obtained using a roughness meter (Surfcorder SE1700 – Kosaka Lab., Piracicaba, São Paulo, Brazil), equipped with a diamond tip having a radius of 0.5 µm and a precision of 0.01 µm. The measurements were taken with a cut-off of 0.250 mm, a reading length of 0.8 mm, and a speed of 0.5 mm/s. Three standardized readings were obtained along reference lines, including one central and two at the ends of the specimens, to ensure accuracy. The arithmetic mean of these measurements was calculated for analysis [18].

2.4.2 Wettability

Wettability (n=10) was assessed using the sessile drop technique, involving the deposition of a 20 µL water droplet on the surface. The contact angle between the water droplet and the surface was measured with a goniometer (Ramé-Hart10.000; Ramé-HartInstrumentCo) along with associated software (DROPimageStandard, Ramé-HartInstrumentCo). Three standardized readings were performed (one central and two at the ends of the specimens) and an arithmetic mean was calculated [19].

2.4.3 Brightness

Brightness (n=10) was analyzed using a gloss meter (ZGM 1120 Glossmeter – Zehnter GmbH Testing Instruments; Switzerland). The surface of the specimen was exposed to a beam of light at angles of 20º, 60º and 85º, and the intensity of the reflected light was measured and compared to a reference value. All specimens were positioned consistently, and four measurements were taken for each specimen, one in each quadrant. An average was calculated for the four measurements as well as for the three measurement angles, resulting in a single value per specimen [20].

2.5 Mechanical characterization

2.5.1 Knoop hardness

The Knoop hardness of the specimens (n=10) was investigated using an indenter (Future-Tech FM Corp., Tokyo, Japan) coupled with software (FM-ARS 9000, Future-Tech FM Corp.). A 10 kgf force was applied for 5 seconds, and three indentations were made on each specimen. The average hardness value was then calculated for each specimen. For each indentation, the following formula was used to compute hardness: $KHN=P/C_pL^2$. Where "KHN" represents Knoop hardness, "P" represents the applied load (kgf), "C_p" represents the correction factor, and "L" represents the length (mm) of the long indentation diagonal [21].

2.5.2 Flexural resistance

Three-point flexural strength (n=20) was conducted using a universal testing machine (Instron Model 4400 Universal Testing System; Instron Corp) by ISO 20795-1:201320. The loading force was uniformly increased from 0 with a constant displacement of 5±1 mm/min until the bar fractured. Flexural strength was calculated using the following formula: $FS=3FL/2bh^2$, where FS represents the flexural strength (MPa), F is the maximum applied force (N), L is the distance between the body support and test (mm), b is the width of the sample (mm) and h is the height of the sample (mm) [11].

2.6 Biofilm formation

Two monospecies biofilm models and one mixed biofilm model were developed over 24 hours to assess the impact of the surface on the viability of bacteria and fungi. For this purpose, strains of *Streptococcus mitis* (S. *mitis*, ATCC 35037) and *Candida albicans* (*C. albicans*, ATCC MYA-2876) were individually reactivated. *S. mitis* was cultivated on Brain Heart Infusion (BHI) medium plates (Becton-Dickinson, USA) supplemented with nystatin (250 U/mL) for 24 hours at 37 °C in a 10% CO_2 atmosphere, while *C. albicans* was incubated at 30 °C on Sabouraud Dextrose Agar medium (Becton-Dickinson, USA) supplemented with chloramphenicol (1 mg/mL). After reactivation, seven colonies of each microorganism were selected and transfered into 10 mL of BHI + glucose broth (9:1) for *S. mitis* and 10 mL of Yeast Extract Peptone (YPD) (Becton-Dickinson, USA) + BHI (7:3) for *C. albicans* for 16 hours. Subsequently, the inoculum was adjusted to an optimal density (OD) of 1.0 at 600 nm, representing a suspension containing 10^7 microbial cells/mL for *S. mitis* and 10^5 for *C. albicans.*

The resin discs were sterilized using UV light (4 W, λ = 280 nm, Osram Ltd., Germany) for 20 minutes on each side. Following sterilization, the discs were placed for biofilm formation (24 h) in a 24-well plate containing 100 µL of *S. mitis* + 100 µL of *C. albicans* + 800 µL of YPD+BHI, incubated under the conditions described above. Subsequently, the discs were washed three times in 0.9% NaCl and transferred to cryogenic tubes containing 1 mL of 0.9% NaCl, where they were shaken in a vortex and sonicated (Branson, Sonifer 50, Danbury, CT, USA) at 7 W for 30 seconds. An aliquot of 100 µL of the sonicated cell suspension was used for serial dilution (7×) in 0.9% NaCl and plated on BHI + Nystatin, SDA + chloramphenicol, and Blood agar plates. Colonyforming units (log CFU/mL) were subsequently counted. Additional biofilm-contaminated discs were used to analyze the biofilm morphology using a SEM (JEOL JSM-6010LA, Japan) operating at 15 kV [22].

2.7 Statistical analysis

Bivariate analyses and simple (crude) and multiple (adjusted) regression were performed. For the bivariate analysis, data normality was assessed using the Kolgomorov-Smirnov test. Due to the lack of normality in the data, the Mann-Whitney test was applied to compare the impact of glaze on the surface of denture base resins concerning surface, mechanical and microbiological properties, with a significance level set at $p<0.05$. Simple (crude) and multiple (adjusted) step-by-step linear regression analyses were performed for the study's dependent and independent variables (denture base resins, glaze and, thermocycling). In the adjusted model, variables with $p<0.2$ in simple regression were included.

3. Results

The application of glaze influenced the surface properties of 3D printed denture base resins compared to heat-polymerized ones. Glazing resulted in reduced surface roughness (B = -0.33; $p<0.001$) and wettability by -8.470º, while brightness increased by 21.30 (gloss unit [GU]). Considering the type of resins for 3D printed denture bases, surface roughness increased for YL (B=0.133; p=0.002) and PX (B=0.044; p=0.307), whereas it remained relatively stable for PZ (B=0.020; p=0.642). PZ resin was associated with increased brightness (B=6.985; p=0.038), while YL (B=-1.605; p=0.634) and PX (B=-3.430; p=0.309) showed reductions in brightness. Furthermore, thermocycling was found to increase surface roughness (B=0.080; p=0.009) while reducing brightness (B=-14.68; $p<0.001$) and wettability (B=-7.805; $p<0.001$) (Tables 2 and 3).

Glazing (B=9.964; $p<0.001$) and thermocycling (B=4.560; p=0.005) were found to increase the hardness of the denture base resins, both heat-polymerized and 3D printed. However, regarding the type of resin for the denture base, the hardness significantly decreased for all 3D printed resins compared to heat-polymerized resins ($p<0.001$). Furthermore, flexural strength was reduced for PX (B=-45.194; $p<0.001$) and YL (B=-31.666; $p<0.001$), while it increased for PZ (B=28.838; $p<0.001$). Notably, neither glazing or thermocycling had a significant impact on flexural strength (Tables 4 and 5).

The glazing of resins for 3D printed denture bases resulted in a significant reduction in *C. albicans* colonization. The heat-polymerized resin exhibited higher colonization of *C. albicans*, showing significant differences compared to the YL, PZ and PX 3D printed resins ($p<0.001$). Notably, the PZ resin had the most significant impact on this reduction, as evidenced in the multiple regression model (B= -10.611; $p<0.001$) (Fig. 2A). As for *S. mitis*, there were no differences observed among the resins for denture bases ($p>0.05$) (Fig. 2B). However, the YL resin demonstrated a noteworthy reduction of -9.472 log CFU/mL (p = 0.012) and the application of glaze (B=-4.498; p=0.035) reduced the colonization of *S. mitis* and *C. albicans* dual-species biofilms for all 3D printed resins compared to heat-polymerized resin (Tables 6-8 and Fig. 2C). SEM images corroborated these findings, showing a reduction in the colonization of both *S. mitis* and *C. albicans* dual-species biofilms after surface glazing (Fig. 3).

4. Discussion

The application of glaze acted as a protective barrier on the 3D printed denture base resins, resulting in a smoother, glossier, less hydrophilic, harder, and more resistant to bending surface compared to heat-polymerized denture base resin. Such changes had a significant impact on reducing the colonization of *C. albicans* and the dual-species biofilm of *S. mitis* and C. *albicans*, when compared to heat-polymerized denture base resin.

It is well-established that roughness plays a crucial role in determining surface hydrophilicity, as it increases the surface area and thereby enhances the affinity of the surface with liquids. In the present study, the observed hydrophilicity can be attributed to the reduction in surface roughness achieved through the application of glaze and thermocycling. The glossier and smoother surface created by glazing increased the contact between the water droplet and the functional groups of the resins (oligomers for 3D printed resins and methylmethacrylate for heat-polymerized resin), consequently increasing the interaction forces [23-25]. In line with our findings, Hahnel et al (2017) [26] reported a decrease in the hydrophobicity of denture base resins decreased after thermal cycling, which can likely be attributed to the modification of residual components of the resin caused by the numerous thermal cycles conducted.

Initially, the hydrophilicity of the resin surface may indeed create conditions favorable for microbiological adhesion. However, it is important to note that the hydrophilicity alone was not decisive for the microbiological outcomes observed in this study. Microbiological adhesion to materials can vary considerably depending on various surface properties [26-30]. Numerous studies have indicated that surface roughness plays a more significant role in microbiological adhesion compared to surface free energy [31,32]. Therefore, a smoother surface on the prosthesis contributes to reducing the adhesion of *C. albicans*. While the roughness values in our study may have exceeded the threshold of 0.2 μm, beyond which surface roughness begins to significantly microbiological adhesion to prosthetic surfaces [33], the substantial reduction in roughness and increase in brightness observed in our study may have justified the microbiological findings.

The significant reduction in *C. albicans* adhesion observed with glazing underscores the efficacy of this technique. However, the porous nature of PMMA (polymethylmethacrylate) in heat-polymerized resins, along with the presence of irregularities and the capacity to absorb organic proteins, justify the greater adhesion observed in this material [34]. In the case of 3D printed resins, the layer-by-layer deposition process inherently results in a rougher surface, albeit one that can be minimized [33,35]. Previous studies have demonstrated that adjustments to printing parameters, layer direction relative to the specimen surfaces, and printing orientations can mitigate surface roughness and even morphological changes in 3D printed resins [36].

Previous studies have identified Streptococcus species from the mitis group as the primary initial colonizers in biofilms formed on dental surfaces [37-39]. These bacteria are often referred to as “accessory pathogens” due to their ability to form multispecies biofilms and increase community virulence [40]. Notably, Streptococcus species have been shown to form robust, hypervirulent biofilms When in conjunction with C. *albicans* [41,42]. Given this understanding, it is plausible that Streptococci possess an increased initial adhesion capacity on the surfaces of denture base resins, thereby limiting opportunities for Candida colonization [37]. Alternatively, it is conceivable that during the later stages of biofilm growth, Streptococci may produce small molecules with antifungal properties in a density-dependent manner [43]. This could potentially explain why pre-formed Streptococcal biofilms on denture base resins did not facilitate Candida growth.

The polishing procedure, associated with the application of glaze, plays a pivotal role in influencing the surface hardness of the resin for denture bases. This is primarily attributed to the significant reduction in defects, such as scratches, which are known to diminish surface hardness [44]. Consequently, the observed decrease in roughness and increase in brightness in our study directly contributed to the enhanced surface hardness of the denture base resins. This finding aligns with the results reported by Choi et al (2020) [1], who also observed an increase in the surface hardness of resin for denture bases coated with glaze.

The difference in hardness results obtained across different types of denture base resins can be attributed to their internal structures. Impression resins typically exhibit lower double-bond conversion rates compared to prostheses manufactured by heat-polymerized and CAD-CAM (milled) resins, which can significantly impact their mechanical properties [9,45]. Furthermore, the positive effect of thermocycling on the hardness of the denture base resins observed in our study can be explained by several factors. During the accelerated aging process, resins undergo water absorption and experience temperature fluctuations. This can lead to an increase in the release of residual monomer, resulting in continued polymerization of the resin. Consequently, higher hardness values are attained due to this ongoing polymerization process [46].

Vertical impression orientation has been demonstrated to yield higher flexural values compared to horizontal orientation for denture base resins [47]. However, our findings revealed a reduction in flexural strength when the glaze was applied to the denture base resins (YL, PZ e CT). This reduction can be attributed to the ability of the glaze to create a surface with greater hardness, effectively forming a type of glazing on the material, which subsequently diminishes its bending capacity. Alternatively, the presence of pendant methacrylate groups in the glaze may act as plasticizers at low strain rates. This plasticizing effect is due to the pendant methacrylate groups that separate the main segments of the chain [47].

The base of the prosthesis must possess high flexural strength to withstand the stresses encountered during cleaning, insertion, or removal, thereby minimizing the risk of resin fractures [48]. A minimum flexural strength value of 65 Mpa has been established for this purpose [49]. Based on our findings, both heat-polymerized and additively manufactured denture base resins (YL and PZ) met or exceeded this threshold. Therefore, it can be concluded that among the 3D printed resins tested, PZ emerges as the safest option for the fabrication of printed prostheses. Its flexural strength values remained within the acceptable range for clinical use, even following artificial aging and glaze application.

The findings of this study highlight the potential benefits of glazing the surface of denture base resins, irrespective of whether they are heat-polymerized or 3D printed. Glazing has been shown to address various clinical issues associated with these materials, including stains or discoloration, surface roughness, brightness, microbiological adhesion, and hardness. Moreover, the glaze utilized in this study is cost-effective, simple to apply, and can be swiftly implemented by dental technicians. As such, glazing represents a promising approach to enhancing the overall performance and longevity of denture base resins in clinical practice.

This study assessed the materials under controlled laboratory conditions, examining a single glaze and several commercially available resins for denture base. Consequently, further research is warranted to explore the impacts of glazes with varying compositions and application methods on denture base resins under oral conditions. Additionally, investigations into the correlation between glazing of denture base resins and susceptibility to discoloration or staining are necessary. Such studies would provide valuable insights into optimizing glazing techniques and materials to enhance the performance and aesthetics of denture prostheses in clinical practice.

5. Conclusion

Within the limitations of this in vitro study, glazing served as a protective barrier in 3D printed denture base resins, resulting in smoother, glossier, hydrophilic, harder, and more resistant surfaces. Such changes had an impact on reducing the colonization of C. albicans and of S. mitis and C. albicans dual-species biofilms compared to heat-polymerized denture base resin, which could clinically modulate biofilm formation. However, longer-lasting surface treatments are still needed in the oral environment, given the impact of thermocycling on the surface properties and hardness of resins for 3D printed denture bases. Given this, among the 3D printed denture base resins examined in this study, Prizma showed superior performance across the properties evaluated.

Declaration of Competing Interest

The authors declare that they have no known competing financial interests or personal relationships that could have appeared to influence the work reported in this paper.

Acknowledgments

The Coordination for the Improvement of Higher Education Personnel (CAPES), Brazil [Finance code 001]. The Piracicaba Dental School – University of Campinas, in particular the Laboratory of Biochemistry, Dental Materials, Total Prosthesis and Pediatric Dentistry, as well as the São Paulo State University for the structure made available to carry out this study. The commercial companies Makertech Labs, Yller Biomaterials and PrintaX for providing the materials used in this study.

6. References

1. Choi JJE, Uy CE, Ramani RS, Waddell JN. Evaluation of surface roughness, hardness and elastic modulus of nanoparticle containing light-polymerized denture glaze materials. J Mech Behav Biomed Mater, 2020; 103:103601.
2. Emmanouil JK, Kavouras P, Kehagias Th. The effect of photo-activated glazes on the microhardness of acrylic baseplate resins. J Dent, 2002; 30:7-10.
3. Sesma N, Laganá DC, Morimoto S, Gil C. Effect of denture surface glazing on denture plaque formation. Braz Dent J, 2005; 16:129-34.
4. Sahin O, Koroglu A, Dede DO, Yilmaz B. Effect of surface sealant agents on the surface roughness and colour stability of denture base materials. J Prosthet Dent, 2016; 116:610-616.
5. Kutlu IU, Yanikoglu ND, Kul E, Duymus ZY. Effect of sealer coating and storage methods on the surface roughness of soft liners. J Prosthet Dent, 2016; 115:371-6.
6. Teixeira ABV, Da Costa Valente ML, Sessa JPN, Gubitoso B, Schiavon MA, Dos Reis AC. The influence of surface roughness and surface-free energy on supra- and subgingival plaque formation in man. A review of the literature. J Adv Prosthodont, 2023; 15:80-92.
7. Choi JJE, Ramani RS, Ganjigatti R, Uy CE, Plaksina P, Waddell JN. Adhesion of Denture Characterizing Composites to Heat-Cured, CAD/CAM and 3D Printed Denture Base Resins. J Prosthodont, 2021; 30:83-90.
8. Alouthah H, Lippert F, Yang C-C, Levon JA, Lin W-S. Comparison of surface characteristics of denture base resin materials with two surface treatment protocols and simulated brushing. J Prosthodont, 2023. Online ahead of print.

9. Choi JJE, Uy CE, Ramani RS, Waddell JN. Evaluation of surface roughness, hardness and elastic modulus of nanoparticle containing light-polymerized denture glaze materials. J Mech Behav Biomed Mater, 2020; 103:103601.
10. Yoshida K, Taira Y, Atsuta M. Properties of opaque resin composite containing coated and silanized titanium dioxide. J Dent Res, 2001; 80: 864-868.
11. Prpić V, Schauperl Z, Ćatić A, et al: Comparison of mechanical properties of 3D-printed, CAD/CAM, and conventional denture base materials. J Prosthodont, 2020; 29:524-528.
12. De Freitas RFCP, Duarte S, Feitosa S, Dutra V, Lin W-S, Panariello BHD, Da Fonte Porto Carreiro A. Physical, Mechanical, and Anti-Biofilm Formation Properties of CAD-CAM Milled or 3D Printed Denture Base Resins: In Vitro Analysis. J Prosthodont, 2023; 32:38-44.
13. Meirowitz A, Rahmanov A, Shlomo E, et al: Effect of denture base fabrication technique on Candida albicans adhesion in vitro. Materials (Basel), 2021; 14:1-8.
14. International Organization for Standardization ISO 20795- 1: 2013. Dentistry – Base polymers- Part 1: Denture base polymers. Geneva: ISO; 2013. pp. 1–42.
15. Consani RLX, Folli BL, Nogueira MCF, Correr AB, Mesquita MF. Effect of Polymerization Cycles on Gloss, Roughness, Hardness and Impact Strength of Acrylic Resins. Braz Dent J, 2016;27:176–80.
16. Melo CBF, Feitosa MD, Maia SDB, Barreto JO, Peixoto RF, Regis RR. Effect of a continuous mechanical polishing protocol on the color stainability, microhardness, mass, and surface roughness of denture base acrylic resin. J Prosthet Dent, 2021; 126:796-802.

17. Çakmak G, Donmez MB, Akay C, Abou-Ayash S, Schimmel M, Yilmaz B. Effect of Thermal Cycling on the Flexural Strength and Hardness of New Generation Denture Base Materials. J Prosthodont, 2023; 32:81-86.
18. Lepri CP, Palma-Dibb RG. Surface roughness and color change of a composite: influence of beverages and brushing. Dent Mater J, 2012; 31:689-96.
19. Al-Dwairi Z, Ebrahim AAAH, Baba NZ. A Comparison of the Surface and Mechanical Properties of 3D Printable Denture-Base Resin Material and Conventional Polymethylmethacrylate (PMMA). J Prosthodont, 2023; 32:40-48.
20. Lassila l, Sailynoja E, Prinssi R, Vallittu PK, Garoushi S. The effect of polishing protocol on surface gloss of different restorative resin composites. Biomater Investig Dent, 2020; 7:1-8.
21. De Castro EF, Nima G, Rueggeberg FA, Giannini M. Effect of build orientation in accuracy, flexural modulus, flexural strength, and microhardness of 3D-Printed resins for provisional restorations. J Mech Behav Biomed Mater, 2022; 136:105479.
22. Dos S. Silva JP, Costa RC, Nagay BE, Borges MHR, Sacramento CM, Da Cruz NC, et al. Boosting titanium surfaces with positive charges: Newly developed cationic coating combines anticorrosive and bactericidal properties for implant application. ACS Biomater Sci Eng, 2023; 9:5389-5404.
23. Elkin B, Mayer J, Schindler B, Vohrer U. Wettability, chemical and morphological data of hydrophobic layers by plasma polymerization on smooth substrates. Surf Coat Technol, 1999; 116–119: 836–40.
24. Nishioka M, Yamabe Y, Hisatsune K, Fujii H. Influence of polishing of denture base resin and metal surfaces on wettability with water and saliva. Dent Mater J, 2006; 25: 161–5.

25. De Foggi CC, Machado AL, Zamperini CA, Fernandes D, Wady AF, Vergani CE. Effect of surface roughness on the hydrophobicity of a denture-base acrylic resin and Candida albicans colonization. J Investig Clin Dent, 7:141-8.
26. Hahnel S, Ionescu AC, Cazzaniga G, Ottobelli M, Brambilla E. Biofilm formation and release of fluoride from dental restorative materials in relation to their surface properties. J Dent, 2017; 60:14–24.
27. Buergers R, Schneider-Brachert W, Hahnel S, Rosentritt M, Handel G. Streptococcal adhesion to novel low-shrink silorane-based restorative. Dent Mater, 2009; 25:269–275.
28. Cazzaniga G, Ottobelli M, Ionescu AC, Paolone G, Gherlone E, Ferracane JL, Brambilla E. In vitro biofilm formation on resin-based composites after different finishing and polishing procedures. J Dent, 2017; 67:43–52.
29. Yuan C, Wang X, Gao X, Chen F, Liang X, Li D. Effects of surface properties of polymer-based restorative materials on early adhesion of Streptococcus mutans in vitro. J Dent, 2016; 54:33–40.
30. Can DB, Dundar A, Barutçugil Ç, Ozyurt OK. Evaluation of surface characteristic and bacterial adhesion of low-shrinkage resin composites. Microsc Res Tech, 2021; 84:1783-1793.
31. Quirynen M, Bollen CM. The influence of surface roughness and surface-free energy on supra-and subgingival plaque formation in man. A review of the literature. J. Clin. Periodontol, 1995; 22:1-14.
32. Quirynen M, Marechal M, Busscher HJ, Weerkamp AH, Darius PL, van Steenberghe D. The influence of surface free energy and surface roughness on early plaque formation: an in vivo study in man. J Clin Periodontol, 1990; 17:138-144.

33. Lee W-J, Jo Y-H, Yilmaz B, Yoon H-I. Effect of build angle, resin layer thickness and viscosity on the surface properties and microbial adhesion of denture bases manufactured using digital light processing. J Dent, 2023; 137:104608.

34. Raszewski Z, Nowakowska-Toporowska A, Nowakowska D, Wieckiewicz W. Update on acrylic resins used in dentistry. Mini Rev Med Chem, 2021; 21:2130-2137.

35. Goodacre BJ, Goodacre CJ. Additive manufacturing for complete denture fabrication: a narrative review. J Prosthodont, 2022; 31:47-51.

36. Al-Qarni FD, Gad MM. Printing accuracy and flexural properties of different 3D-printed denture base resins. Materials, 2022; 15:2410.

37. Rickard AH, Gilbert P, High NJ, Kolenbrander PE, Handley PS. 2003. Bacterial coaggregation: an integral process in the development of multi-species biofilms. Trends Microbiol, 2003; 11:94 –100.

38. Diaz PI, Chalmers NI, Rickard AH, Kong C, Milburn CL, Palmer RJ, Jr, Kolenbrander PE. Molecular characterization of subject-specific oral microflora during initial colonization of enamel. Appl Environ Microbiol, 2006; 72:2837–2848.

39. Diaz PI, Dupuy AK, Abusleme L, Reese B, Obergfell C, Choquette L, Dongari-Bagtzoglou A, Peterson DE, Terzi E, Strausbaugh LD. Using high throughput sequencing to explore the biodiversity in oral bacterial communities. Mol Oral Microbiol, 2012; 27:182–201.

40. Whitmore SE, Lamont RJ. The pathogenic persona of community associated oral streptococci. Mol Microbiol, 2011; 81:305–314.

41. Diaz PI, Xie Z, Sobue T, Thompson A, Biyikoglu B, Ricker A, Ikonomou L, Dongari-Bagtzoglou A. Synergistic interaction between Candida albicans and

commensal oral streptococci in a novel in vitro mucosal model. Infect Immun, 2012; 80:620-632.

42. Xu H, Sobue T, Thompson A, Xie Z, Poon K, Ricker A, Cervantes J, Diaz PI, Dongari-Bagtzoglou A. Streptococcal co-infection augments Candida pathogenicity by amplifying the mucosal inflammatory response. Cell Microbiol, 2014; 16:214-231.
43. Souza JGS, Bertolini M, Thompson A, Barão VAR, Dongari-Bagtzoglou A. Biofilm interactions of candida albicans and mitis group streptococci in a titanium-mucosal interface model. Appl Environ Microbiol, 2020; 86:e02950-19.
44. Dede DO, Sahin O, Koroglu A, Yilmaz B. Effect of sealant agents on the color stability and surface roughness of nanohybrid composite resins. J Prosthet Dent, 2016; 116:119-28.
45. Al-Dulaijan YA, Alsulaimi L, Alotaibi R, Alboainain A, Alalawi H, Alshehri S, Khan SQ, Alsaloum M, AlRumaih HS, Alhumaidan AA, Gad MM. Comparative Evaluation of Surface Roughness and Hardness of 3D Printed Resins. Materials (Basel), 2022; 15:6822.
46. Dos Santos, DM, Nagay BE, Da Silva EVF, Da Rocha Bonatto L, Sonego MV, Moreno A, Rangel EC, Da Cruz NC, Goiato MC. In vitro analysis of different properties of acrylic resins for ocular prosthesis submitted to accelerated aging with or without photopolymerized glaze. Mater Sci Eng C Mater Biol Appl, 2016; 1:995-1003.
47. Ruyter IE, Svendsen SA. Flexural properties of denture base polymers. J Prosthet Dent, 1980; 43:95-104.

48. Chhabra M, Kumar MN, RaghavendraSwamy KN, Thippeswamy HM. Flexural strength and impact strength of heat-cured acrylic and 3D printed denture base resins- A comparative in vitro study. J Oral Biol Craniofac Res, 2022; 12:1-3.
49. Gad MM, Fouda SM, Abualsaud R, Alshahrani FA, Al-Thobity AM, Khan SQ, Akhtar S, Ateeq LS, Helal MA, Al-Harbi FA. Strength and Surface Properties of a 3D-Printed Denture Base Polymer. Journal of Prosthodontics. J Prosthodont, 2022; 31:412-418.

Captions to tables and figures

Table 1. Materials used in the study.

Table 2. Effect of glaze on the surface properties of denture base resins (heat-polymerizable and 3D printed).

Table 3. Influence of the type of resin, glaze and thermocycling on surface properties.

Table 4. Effect of glaze on the mechanical properties of denture base resins (heat-polymerized and 3D printed).

Table 5. Influence of the type of resin, glaze and thermocycling on mechanical properties.

Table 6. Comparison between denture base resins for each microbiological strain (Log CFU/mL).

Table 7. Influence of the type of resin, glaze and thermocycling on microbiological properties (Log CFU/mL).

Figure 1. Study flowchart.

Figure 2. Biofilm growth of Candida *albicans* (A), Streptococcus *mitis* (B) and S. *mitis* and C. *albicans* dual-species (Log CFU/mL) in twenty-four hours (C).

Figure 3. Growth of S. *mitis* and C. *albicans* dual-species after twenty-four hours on heat-polymerizable (CT) and 3D printed resins (PrintaX [PX], Prizma [PZ] and Yller [YL]) unglazed and glazed.

Table 1. Materials used in the study.

Commercial name	Composition	Manufacturer
VIPICRIL Plus	Polymer (polymethyl methacrylate, polypropylene, pigments) Monomer (methylmethacrylate, EDMA – crosslink, inhibitor)	VIPI, Pirassununga, São Paulo, Brazil
PRIZMA 3D Bio Prov	Proprietary acrylate and triacrylated monomers (>10%), amorphous silica (≤5%), fillers – proprietary (<10%), proprietary meta-acrylated oligomers (<70%), diphenyl (2,4,6-trimethylbenzoyl)-phosphine oxide (<5%)	Makertech, Tatuí, São Paulo, Brazil
PrintaX BB Base	Aromatic methacrylic oligomer (<80%), aliphatic methacrylic oligomer (<30%), phosphine oxide (<5%)	PrintaX, Ribeirão Preto, São Paulo, Brazil
Cosmos Denture	Oligomers, monomers, photoinitiators, stabilizer and pigment	Yller Biomateriais, Pelotas, Rio Grande do Sul, Brazil
Glaze Megaseal	Methylmethacrylate (MMA), epoxiliertes bisphenol A dimethacrylat, 2,4,6-trimethyl-benzoyl-diphenylphosphinoxid, 2-(2-hydroxy-5-methylphenyl)benzotriazol	OdontoMega, Ribeirão Preto, São Paulo, Brazil

Table 2. Effect of glaze on the surface properties of denture base resins (heat-polymerizable and 3D printed).

Groups	Presence or absence of surface change of the resin	Surface Roughness (Ra)						
		Without Thermocycling			With Thermocycling		Overall	
		n	Med (Q^{25-75})	p	Med (Q^{25-75})	p	Med (Q^{25-75})	p
CT	**Unglazed**	10	0.4496 (0.3650-0.5089)	<0.001	0.3498 (0.2696-0.3652)	0.007	0.3651 (0.3286-0.4496)	<0.001
	Glazed	10	0.1061 (0.0637-0.1423)		0.2548 (0.1694-0.2682)		0.1572 (0.1005-0.2548)	
YL	**Unglazed**	10	0.6500 (0.6216-0.6967)	<0.001	0.5342 (0.5215-0.5623)	<0.001	0.6067 (0.5342-0.6500)	<0.001
	Glazed	10	0.1974 (0.1831-0.2065)		0.2346 (0.2061-0.2440)		0.2063 (0.1905-0.2346)	
PZ	**Unglazed**	10	0.3100 (0.2794-0.3547)	<0.001	0.5439 (0.4943-0.6057)	<0.001	0.4315 (0.3100-0.5439)	<0.001
	Glazed	10	0.0652 (0.0569-0.0766)		0.2279 (0.1994-0.2583)		0.1391 (0.0652-0.2279)	
PX	**Unglazed**	10	0.4200 (0.4064-0.4473)	<0.001	0.6236 (0.6063-0.6801)	<0.001	0.5033 (0.4200-0.6236)	<0.001
	Glazed	10	0.0571 (0.0528-0.0579)		0.1482 (0.1368-0.1692)		0.0913 (0.0571-0.1482)	

Groups	Presence or absence of surface change of the resin	Brightness (Gloss unit [GU])						
		Without Thermocycling			With Thermocycling		Overall	
		n	Med (Q^{25-75})	p	Med (Q^{25-75})	p	Med (Q^{25-75})	p
CT	**Unglazed**	10	73.4000 (73.1000-73.8000)	<0.001	60.7500 (57.1000-63.0000)	<0.001	68.3500 (60.7500-73.4000)	<0.001
	Glazed	10	85.0500 (84.8000-85.3000)		74.3000 (72.2000-74.8000)		80.3500 (74.3000-85.0500)	
YL	**Unglazed**	10	72.8500 (72.7000-73.1000)	<0.001	49.9500 (45.7000-52.5000)	<0.001	62.7000 (49.9500-72.8500)	<0.001
	Glazed	10	84.0500 (80.0000-85.3000)		80.7500 (78.4000-82.0000)		81.5500 (79.8000-84.0500)	
PZ	**Unglazed**	10	73.6500 (73.0000-74.1000)	<0.001	69.8500 (69.0000-70.7000)	<0.001	72.1500 (69.8500-73.6500)	<0.001
	Glazed	10	95.3500 (95.1000-95.7000)		81.2000 (80.3000-81.7000)		88.7500 (81.2000-95.3500)	
PX	**Unglazed**	10	73.2500 (72.0000-74.0000)	<0.001	29.5500 (28.9000-29.8000)	<0.001	55.8000 (29.5500-73.2500)	<0.001
	Glazed	10	90.3000 (89.4000-91.8000)		83.9500 (82.9000-85.3000)		87.6000 (83.9500-90.3000)	

Groups	Presence or absence of surface change of the resin	Wettability (º)						
		Without Thermocycling			With Thermocycling		Overall	
		n	Med (Q^{25-75})	p	Med (Q^{25-75})	p	Med (Q^{25-75})	p
CT	**Unglazed**	10	93.8800 (90.2600-96.9600)	<0.001	96.1100 (94.5600-96.8300)	<0.001	95.3150 (93.4100-96.8950)	<0.001
	Glazed	10	75.9000 (74.3300-81.1000)		69.9300 (62.6300-81.6700)		75.0150 (69.9300-81.6700)	
YL	**Unglazed**	10	95.5650 (93.4600-97.0000)	<0.001	74.6100 (73.4300-76.6300)	0.821	85.8150 (74.6100-95.5650)	0.204
	Glazed	10	84.1500 (83.8300-85.1300)		74.8300 (74.7000-75.0000)		79.3950 (74.8300-84.1500)	
PZ	**Unglazed**	10	83.6950 (79.0000-86.1000)	<0.001	78.9300 (77.6000-80.1000)	0.307	79.9500 (78.0000-83.6950)	<0.001
	Glazed	10	75.0000 (74.5300-76.0300)		77.7150 (76.8300-79.5600)		76.0800 (74.7650-77.7150)	
PX	**Unglazed**	10	94.3950 (86.4600-94.6600)	<0.001	75.6650 (72.8600-76.1000)	0.016	81.9100 (75.6650-94.3950)	0.045
	Glazed	10	85.1150 (84.0600-86.3600)		73.0300 (71.4000-73.5600)		78.3450 (73.0300-85.1150)	

Med (Median); Q^{25-75} (Quatile 25 and 75); CT (heat-polymerized denture base resin); YL (3D printed denture base resin – YLLER); PZ (3D printed denture base resin – PRIZMA); PX (3D printed denture base resin – PRINTAX).

Table 3. Influence of the type of resin, glaze and thermocycling on surface properties.

				Surface Roughness (Ra)				
			Crude (RAW)			Adjusted		
		n	B	CI 95%	p	B	CI 95%	p
3D printed denture base resin	PX	40	0,04	(-0.040 – 0.012)	0.307	0.044	(0.005 – 0.082)	0.026
	PZ	40	0,02	(-0.064 – 0.103)	0.642	0.020	(-0.018 – 0.058)	0.311
	YL	40	0,13	(0.050 – 0.217)	0.002	0.133	(0.095 – 0.171)	<0.001
Glazed		80	- 0.33	(-0.363 - -0.295)	<0.001	-0.33	(-0.359- -0.299)	<0.001
With thermocycling		80	0.08	(0.020–0.140)	0.009	0.080	(0.050–0.110)	<0.001
							R2=0.753	
				Brightness (Gloss unit [GU])				
		n	B	CI 95%	p	B	CI 95%	p
3D printed denture base resin	PX	40	-3.430	(-10.033 – 3.173)	0.309	-3.430	(-6.820 - - 0.040)	0.047
	PZ	40	6.985	(0.382 – 13.588)	0.038	6.985	(3.595 – 10.375)	<0.001
	YL	40	-1.605	(-8.208 – 4.998)	0.634	-1.605	(-4.995 – 1.785)	0.353
Glazed		80	21.304	(17.78– 24.82)	<0.001	21.30	(18.57–24.03)	<0.001
With thermocycling		80	-14.68	(-18.93- -10.42)	<0.001	-14.68	(-17.41- -11.93)	<0.001
							R2=0.686	
				Wettability (º)				
		n	B	CI 95%	p	B	CI 95%	p
3D printed denture base resin	PX	40	-2.340	(-6.503 – 1.822)	0.270	-2.340	(-5.203 – 0.522)	0.109
	PZ	40	-4.511	(-8.674 - -0.349)	0.034	-4.511	(-7.374 - -1.649)	0.002
	YL	40	-0.772	(-4.934 – 3.390)	0.716	-0.772	(-3.635 – 2.090)	0.597
Glazed		80	-8.47	(-10.854 - - 6.085)	<0.001	-8.470	(-10.470 - - 6.469)	<0.001
With thermocycling		80	-7.805	(-10.245 - - 5.366)	<0.001	-7.805	(-9.806 - - 5.805)	<0.001
							R2=0.460	

CT (heat-polymerized denture base resin); YL (3D printed denture base resin – YLLER); PZ (3D printed denture base resin – PRIZMA); PX (3D printed denture base resin – PRINTAX). The reference for comparison is CT (for denture base resins); Unglazed (for treatment on the surface of the resin for the denture base); without thermocycling (for aging).

Table 4. Effect of glaze on the mechanical properties of denture base resins (heat-polymerized and 3D printed).

Groups	Presence or absence of surface change of the resin	Microhardness (HK)					
		Without Thermocycling		With Thermocycling		Overall	
		Med (Q^{25-75})	p	Med (Q^{25-75})	p	Med (Q^{25-75})	p
CT	**Unglazed**	26.4016 (25.7833-26.9033)	<0.001	53.5733 (51.1400-56.1100)	0.762	37.7333 (26.4016-53.5733)	0.055
	Glazed	48.2100 (46.9866-52.8166)		53.4483 (49.0066-54.8500)		51.0500 (47.2566-54.6333)	
YL	**Unglazed**	23.8066 (22.9200-25.9500)	<0.001	39.7866 (36.2033-43.6233)	0.001	32.2050 (23.8066-39.7866)	0.051
	Glazed	43.1466 (40.3433-46.0033)		34.0200 (33.1200-35.7666)		36.2783 (34.0200-43.1466)	
PZ	**Unglazed**	20.1516 (18.7133-21.8800)	<0.001	35.8266 (34.7466-36.7633)	0.325	28.2800 (20.1516-35.8266)	0.001
	Glazed	36.4116 (34.4266-38.1833)		36.7200 (34.3300-38.8200)		36.7200 (34.3783-38.5016)	
PX	**Unglazed**	37.1600 (34.9900-39.2066)	<0.001	30.7700 (29.8300-35.7400)	0.021	35.1483 (30.2050-38.3166)	<0.001
	Glazed	49.6550 (47.7000-51.9100)		38.2800 (32.5800-41.7100)		42.5766 (38.2800-49.9933)	

Groups	Presence or absence of surface change of the resin	Flexural Strength (MPa)					
		Without Thermocycling		With Thermocycling		Overall	
		Med (Q^{25-75})	p	Med (Q^{25-75})	p	Med (Q^{25-75})	p
CT	**Unglazed**	93.22 (87.99 – 99.18)	0.003	85.70 (80.71 – 89.21)	0.262	88.87 (84.83 – 95.44)	0.005
	Glazed	83.20 (77.38 – 92.71)		83.04 (75.81 – 88.22)		83.04 (76.98 – 88.92)	
YL	**Unglazed**	69.51 (59.64 – 73.99)	< 0.001	42.52 (40.85 – 45.18)	< 0.001	51.63 (42.50 – 69.59)	0.729
	Glazed	47.22 (41.37 – 50.69)		63.82 (58.96 – 68.79)		56.81 (47.22 – 63.82)	
PZ	**Unglazed**	128.84 (125.79 – 132.66)	< 0.001	96.52 (88.19 – 116.08)	< 0.001	120.28 (95.81 – 129.99)	0.870
	Glazed	65.16 (59.48 – 78.55)		167.29 (150.70 – 182.79)		107.32 (64.93 – 168.40)	
PX	**Unglazed**	40.36 (35.46 – 47.35)	0.117	37.47 (34.29 – 41.08)	< 0.001	39.30 (35.36 – 43.44)	0.018
	Glazed	38.44 (35.74 – 41.16)		50.07 (44.05 – 54.69)		42.78 (38.44 – 50.07)	

Med (Median); Q^{25-75} (Quatile 25 and 75); CT (heat-polymerized denture base resin); YL (3D printed denture base resin – YLLER); PZ (3D printed denture base resin – PRIZMA); PX (3D printed denture base resin – PRINTAX).

Table 5. Influence of the type of resin, glaze and thermocycling on mechanical properties.

Microhardness (HK)								
				Crude (RAW)			Adjusted	
		n	B	CI 95%	p	B	CI 95%	p
3D printed denture base resin	PX	40	-6.775	(-10.803 - -2.747)	0.001	-6.775	(-10.155 - -3.395)	<0.001
	PZ	40	-13.459	(-17.487 - -9.432)	<0.001	-13.459	(-16.839 - -10.079)	<0.001
	YL	40	-9.890	(-13.917 - -5.862)	< 0.001	-9.890	(-13.270 - -6.510)	<0.001
Glazed		80	9.964	(6.054 – 11.873)	<0.001	8.820	(6.460 – 11.210)	<0.001
With thermocycling		80	4.560	(1.407 – 7.712)	0.005	4.703	(2.313 – 7.093)	<0.001
							R2 = 0.295	
Flexural Strength (MPa)								
				Crude (RAW)			Adjusted	
		n	B	CI 95%	p	B	CI 95%	p
3D printed denture base resin	PX	40	-45.194	(-51.938 - -38.450)	<0.001	-45.194	(-51.831 - - 38.557)	<0.001
	PZ	40	28.838	(22.094 – 35.581)	<0.001	28.838	(22.201 – 35.475)	<0.001
	YL	40	-31.666	(-38,409 - -24.922)	<0.001	-31.666	(-38.303 - -25.029)	<0.001
Glazed		80	0.192	(-7.705 – 8.088)	0.962	-	-	-
With thermocycling		80	7.713	(-0.138 – 15.564)	0.054	7.713	(2.394 – 3.020)	0.001
							R2=0.066	

CT (heat-polymerized denture base resin); YL (3D printed denture base resin – YLLER); PZ (3D printed denture base resin – PRIZMA); PX (3D printed denture base resin – PRINTAX). The reference for comparison is CT (for denture base resins); Unglazed (for treatment on the surface of the resin for the denture base); without thermocycling (for aging).

Table 6. Comparison between denture base resins for each microbiological strain (Log CFU/mL).

		p-value					
Presence or absence of surface change of the resin	**Biofilms**	**CT x YL**	**CT x PZ**	**CT x PX**	**YL x PZ**	**YL x PX**	**PZ x PX**
Unglazed	C. *albicans*	<0.001	0.757	0.156	0.001	<0.001	0.479
	S. *mitis*	0.825	0.724	0.565	0.825	0.508	0.626
	S. *mitis* and C. *albicans* dual-species biofilms	<0.001	0.791	0.724	<0.001	0.005	0.566
Glazed	C. *albicans*	0.001	<0.001	0.002	<0.001	0.690	<0.001
	S. *mitis*	0.047	0.536	0.157	0.353	0.757	0.596
	S. *mitis* and C. *albicans* dual-species biofilms	0.170	0.894	0.132	0.377	0.310	0.185

CT (heat-polymerized denture base resin); YL (3D printed denture base resin – YLLER); PZ (3D printed denture base resin – PRIZMA); PX (3D printed denture base resin – PRINTAX).

Table 7. Influence of the type of resin, glaze and thermocycling on microbiological properties (Log CFU/mL).

				C. *albicans*				
				Crude (RAW)			Adjusted	
		n	B	CI 95%	p	B	CI 95%	p
3D printed denture base resin	PX	18	-4.361	(-9.021 – 0.299)	0.067	-4.361	(-8.265 - -0.457)	0.029
	PZ	18	-10.611	(-15.271 - -5.951)	<0.001	-10.611	(-14.515 - - 6.707)	<0.001
	YL	18	-9.722	(-14.383 - -5.062)	<0.001	-9.722	(-13.626 - -5.818)	<0.001
Glazed		36	-7.792	(-11.299 - -4.289)	<0.001	-7.792	(- 10.552 - -5.031)	<0.001
							R2=0254	
				S. *mitis*				
				Crude (RAW)			Adjusted	
		n	B	CI 95%	p	B	CI 95%	p
3D printed denture base resin	PX	18	-2.056	(-17.030 – 12.918)	0.788			
	PZ	18	6.417	(-8.557 – 21.391)	0.401			
	YL	18	-5.761	(-20.735 – 9.213)	0.451			
Glazed		36	8.082	(-1.133 – 17.296)	0.085			
				S. *mitis* and C. *albicans* dual-species biofilms				
				Crude (RAW)			Adjusted	
		n	B	CI 95%	p	B	CI 95%	p
3D printed denture base resin	PX	18	-4.361	(-11.708 – 2.986)	0.245	-4.361	(-11.675 – 2.953)	0.243
	PZ	18	2.972	(-4.375 – 10.319)	0.428	2.972	(-4.342 – 10.286)	0.426
	YL	18	-9.472	(-16.819 - -2.125)	0.012	-9.472	(-16.786 - -2.158)	0.011
Glazed		36	-4.498	(-8,663 - -0,332)	0.035	-2.125	(-7.297 – 3.047)	0.421
							R2=0.124	

CT (heat-polymerized denture base resin); YL (3D printed denture base resin – YLLER); PZ (3D printed denture base resin – PRIZMA); PX (3D printed denture base resin – PRINTAX). The reference for comparison is CT (for denture base resins); Unglazed (for treatment on the surface of the resin for the denture base); without thermocycling (for aging).

FIGURES

Figure 1. Study flowchart.

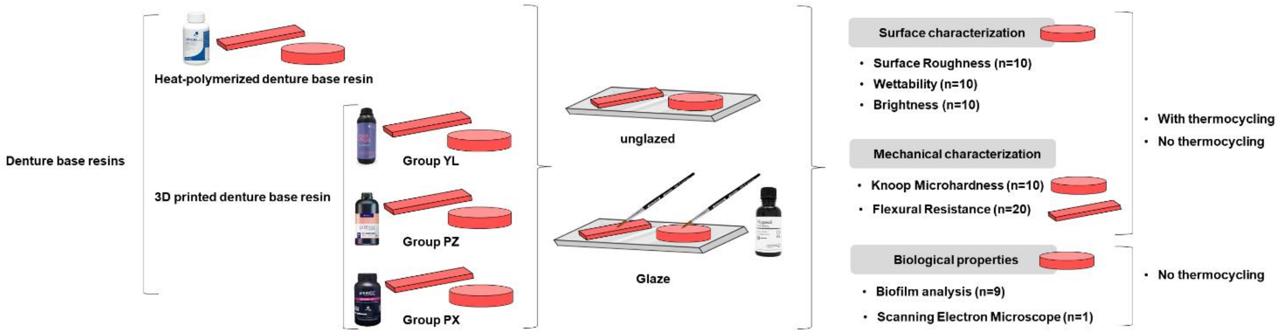

Figure 2. Biofilm growth of Candida *albicans* (A), Streptococcus *mitis* (B) and S. *mitis* and C. *albicans* dual-species (Log CFU/mL) in twenty-four hours (C).

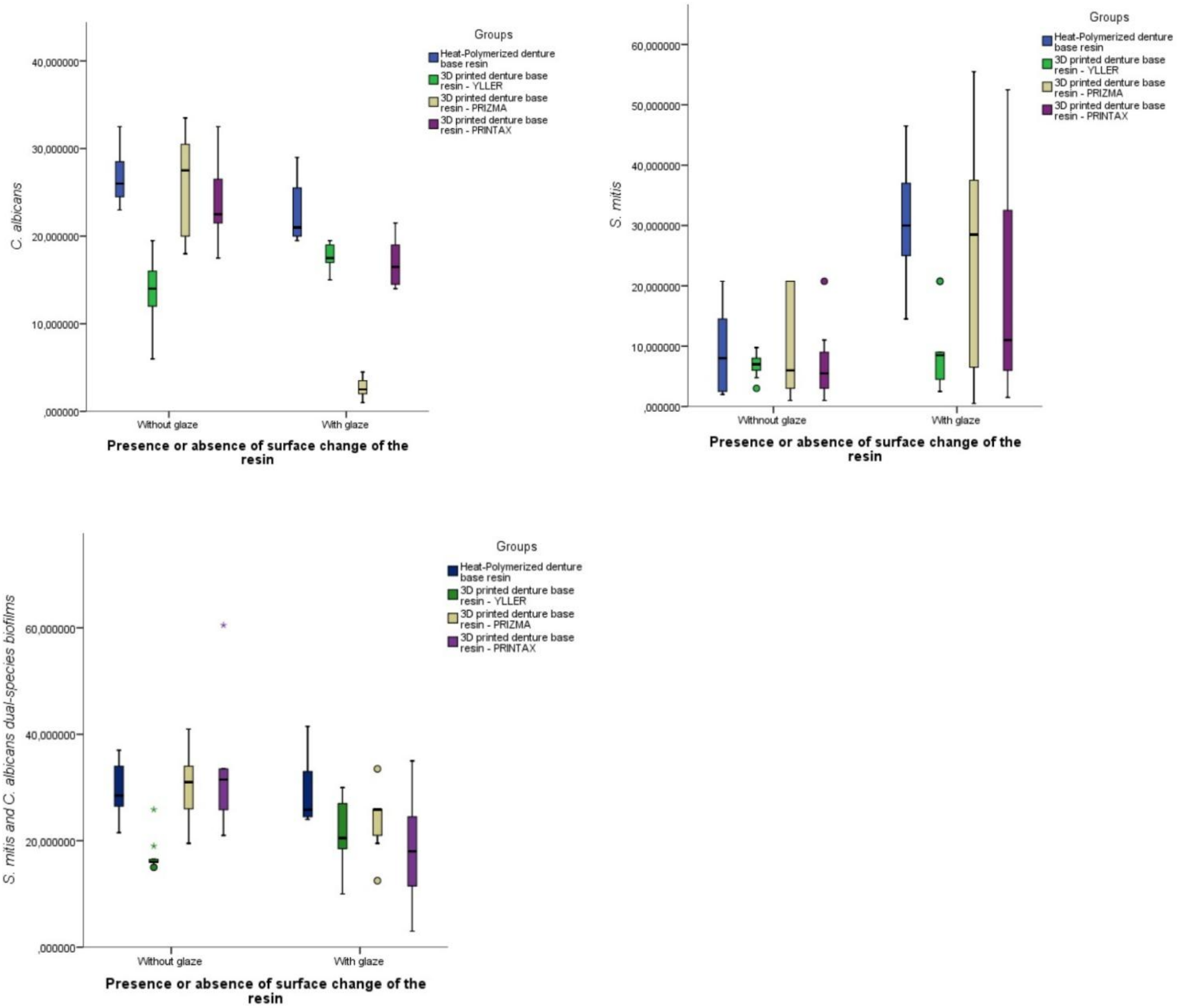

Figure 3. Growth of S. *mitis* and C. *albicans* dual-species after twenty-four hours on heat-polymerizable (CT) and 3D printed resins (PrintaX [PX], Prizma [PZ] and Yller [YL]) unglazed and glazed.